

AD-777 458

ADVANCED MARINE TECHNOLOGY

Allan E. May, et al

Scripps Institution of Oceanography

Prepared for:

Office of Naval Research
Advanced Research Projects Agency

31 December 1973

DISTRIBUTED BY:

NTIS

National Technical Information Service
U. S. DEPARTMENT OF COMMERCE
5285 Port Royal Road, Springfield Va. 22151

Unclassified

SECURITY CLASSIFICATION OF THIS PAGE (When Data Entered)

REPORT DOCUMENTATION PAGE		READ INSTRUCTIONS BEFORE COMPLETING FORM
1. REPORT NUMBER SIO Reference No. 74-7	2. GOVT ACCESSION NO.	3. RECIPIENT'S CATALOG NUMBER AD-777 458
4. TITLE (and Subtitle) Advanced Marine Technology		5. TYPE OF REPORT & PERIOD COVERED 6/1/73-12/31/73 Technical Progress
7. AUTHOR(s) Allan E. May - Part I William G. Van Dorn & Stephan E. Pazan - Part II		6. PERFORMING ORG. REPORT NUMBER AOEL Report No. 47
9. PERFORMING ORGANIZATION NAME AND ADDRESS Scripps Institution of Oceanography University of California, San Diego La Jolla, Ca. 92037 (714) 453-2000 X2476		8. CONTRACT OR GRANT NUMBER(s) N00014-69-A-0200-6012
11. CONTROLLING OFFICE NAME AND ADDRESS Advanced Research Projects Agency 1400 Wilson Boulevard Arlington, Virginia 22217		10. PROGRAM ELEMENT, PROJECT, TASK AREA & WORK UNIT NUMBERS NR 294-016
14. MONITORING AGENCY NAME & ADDRESS (if different from Controlling Office) Office of Naval Research 800 N. Quincy Street Arlington, Virginia 22217		12. REPORT DATE December 1973
		13. NUMBER OF PAGES 30
		15. SECURITY CLASS. (of this report) Unclassified
		15a. DECLASSIFICATION/DOWNGRADING SCHEDULE
16. DISTRIBUTION STATEMENT (of this Report) Distribution of this document is unlimited		
17. DISTRIBUTION STATEMENT (of the abstract entered in Block 20, if different from Report)		
18. SUPPLEMENTARY NOTES Reproduced by NATIONAL TECHNICAL INFORMATION SERVICE U S Department of Commerce Springfield VA 22151		
19. KEY WORDS (Continue on reverse side if necessary and identify by block number) Stable Floating Platform Floating Airfield Seawater Absorption by Concrete Wave Breaking in Deep Water Pitchpoling		
20. ABSTRACT (Continue on reverse side if necessary and identify by block number) This semi-annual report reflects the technical status of projects conducted within the Advanced Ocean Engineering Laboratory at Scripps Institution of Oceanography, Contract No. N00014-69-A-0200-6012. I. <u>Stable Floating Platform</u> - the period from July to December 1973 saw considerable progress in several areas, most notably (A) the 1/8 scale major module (barge), two legs and six struts were fitted out, taken to sea, assembled and disassembled. Tests		

DDC
RECEIVED
APR 19 1974
RECEIVED
D

DD FORM 1473
1 JAN 73EDITION OF 1 NOV 68 IS OBSOLETE
S/M 0102-014-6801

Unclassified

1 < SECURITY CLASSIFICATION OF THIS PAGE (When Data Entered)

Unclassified

SECURITY CLASSIFICATION OF THIS PAGE(When Data Entered)

were highly successful. (B) Reports were issued on the Parametric Study of A Column-Supported Floating Airfield and on Seawater Absorption by Precast Portland Cement Concrete Containing Lightweight Aggregate. (C) Analysis was conducted and reports nearing completion covering various instrumented tests of 1/100 and 1/8 scale models.

II. Wave Breaking In Deep Water - Work during the past six months was divided into two phases. The first phase was a continuation of previous work, examining in greater detail the transformations of internal velocity fields and profiles of periodic waves forcibly "squeezed" to the breaking point within a convergent channel. By comparing consecutive profiles and velocity contour plots, it is apparent that characteristics which distinguish wave approaching the breaking point from symmetric, steady-state, limiting-height waves of the Stokes type are confined to the terminal 80% of wave growth, and to the region beneath the crest above the still water level. Marked asymmetry, leading to a plunging jet, involves very steep velocity gradients within the uppermost 10% of crest height. Crest particle velocities are sometimes accelerated from phase velocity to 60% higher in less than 1/5 wave period. A brief, but illuminating series of pitchpoling experiments with representative model ship hull forms reveals that pitchpoling can only occur when ship-wave interaction occurs very close to the instant of breaking, and if the wave height exceeds overall hull length. A model discus buoy was successfully prevented from pitchpoling by suspending a weight equal to 1/10th its displacement from a central cord five diameters beneath the buoy.

The second phase of our experiments involved interactive breaking of bi-harmonic waves in a non-convergent channel, in which shear flow beneath breaking crests was examined by videotaping shadowgraphs produced by injected dye. It was found that dye blobs in sub-critical, non-breaking waves orbited circularly without much change in shape during a wave period. In steep, near-breaking waves, the dye blob was streaked out along the surface to a length about three times the wave height, and its centroid translated in the wave direction by about half this distance. Despite these intense shearing motions, observations of neutrally buoyant ping-pong balls just beneath the crest revealed little tendency to rotate, although the balls were bodily translated similarly with the dye.

2<

Unclassified

SECURITY CLASSIFICATION OF THIS PAGE(When Data Entered)

Disclaimer

The views and conclusions contained in this document are those of the authors and should not be interpreted as necessarily representing the official policies, either expressed or implied, of the Advanced Research Projects Agency or the U. S. Government

ADVANCED OCEAN ENGINEERING LABORATORY

TECHNICAL PROGRESS REPORT

Table of Contents

Stable Floating Platform	Part I
Wave Breaking in Deep Water	Part II

Part I

STABLE FLOATING PLATFORM

Principal Investigator
Dr. Fred N. Spiess
Phone (714) 453-2000, Extension 2476

ADVANCED OCEAN ENGINEERING LABORATORY

Sponsored by

ADVANCED RESEARCH PROJECTS AGENCY

STRATEGIC TECHNOLOGY OFFICE

ONR Contract N00014-69-A-0200-6012

Part I
STABLE FLOATING PLATFORM

<u>Table of Contents</u>	Page
I. Project Summary	1
II. 1/8 Scale Assembly and Tests	1
III. Parametric Analysis of a Large Platform	2
IV. Water Absorption in Concrete	2
V. References	3
Appendix	4

List of Figures	
Figure 1. Load Cell Locations	. 6

I. Project Summary

During July to December 1973, most appreciable progress has been made on the SIO-Stable Floating Platform Project. Major milestones have been met except for final reports to ARPA which are being submitted in early calendar 1974.

The 1/8 scale major module (barge), two legs and six struts were fitted out, then taken to sea, assembled and disassembled. Tests were highly successful.

An abridged report (reference a) of the Parametric Study of Large Array Platform Components was submitted to ARPA for wider distribution than the original detailed report submitted in reference b.

A report of the study of water absorption in lightweight concrete has been completed (reference c).

Analysis was conducted and reports almost completed covering various instrumented tests of 1/100 scale and 1/8 scale models. DEC PDP-8/E primarily and IBM 1108 computers were used in data collection and analysis. The analysis of force/motion data from the September Sea Trials is almost completed. A report thereof will be shortly included in appropriate final reports.

This is the final semi-annual report for the ARPA Stable Platform Project.

II. 1/8 Scale Assembly and Tests

The fitting out and tests of the 1/8 scale barge, and two legs at sea took the better part of July, August and September 1973. The original plan for summer testing of the complex included (1) in the harbor, (2) at Lake San Vicente (a reservoir), and finally (3) at sea.

As testing progressed, intertwined crane problems and finances precluded the calm water phase at the lake. Instead, a maximum was accomplished in San Diego Harbor. This included flipping the barge with deck load of legs and struts. Also included was separation of a single leg with an upper and lower strut attached. No actual assembly was attempted in the harbor. In spite of heavy tidal currents and summer boat traffic, the in-harbor tests were quite successful.

In August and September tests were conducted at sea in naval operating areas off Coronado, California. An interim report was made in reference d. Full assembly and disassembly were accomplished in August. This commenced with just one leg and two struts to prove the feasibility of rigging procedures.

The final test at sea was conducted in September. After assembly, instrumentation was installed including load cells, accelerometers and wave measuring devices. A computer and other recording devices in a support ship collected the data (see Appendix). Limited analysis was conducted at sea. Results of analysis of force/motion/wave data will be included in various reports still to be submitted.

III. Parametric Analysis of a Large Platform

As the work on the Stable Floating Platform project progressed, it became apparent that a detailed parametric analysis of the more important design/construction considerations would contribute significantly to ultimate project objectives. This was accomplished by L. R. Glosten and Associates for SIO as reported in the last semi-annual report (reference e). ARPA approved an abridgment of the parametric study to be prepared for wider distribution than the original. It was routed to activities and individuals with an interest in floating platforms in reference a.

One of the major conclusions was that of the two leg spacings studied, 200 and 333.3 feet, the larger was more cost effective. The spacing of the 1/8 scale model complex reflected this where the selected spacing between vertical units was 310 feet full scale (38.75 feet for 1/8 scale).

IV. Water Absorption in Concrete

One long-pending item now resolved was a study of seawater absorption by ASTM Type 2 Portland Cement with several different commercially available lightweight aggregates. The basic study was accomplished by Naval Civil Engineering Laboratory at SIO request. A major conclusion from the report was that careful control of manufacturing processes would be most important. This would be especially true for column-stabilized platforms where payload is a small fraction of the structural weight. An edited report has been distributed (reference c).

V. References

- a. SIO Reference Number 73-36, AOEL No. 48, Abridged Parametric Study of A Column-Supported Floating Airfield by L. R. Glosten and Associates.
- b. AOEL Letter Serial No. 721 of 11 April 1973 forwarding "Detailed Parametric Study of Large Array Platform Components by L. R. Glosten and Associates.
- c. SIO Reference Number 73-41, AOEL No. 54, Seawater Absorption by Precast Portland Cement Concrete Containing Lightweight Aggregate by William R. Lorman of Naval Civil Engineering Laboratory.
- d. AOEL Letter Serial No. 825 of 11 September 1973 by F. N. Spiess. (Informal Report of Results of 1/8 Scale Stable Floating Platform Assembly Tests at Sea in August 1973)
- e. SIO Reference Number 73-21, AOEL No. 42, Technical Progress Report. (Stable Floating Platform section)

APPENDIX

September 12, 1973

S/N 829

SUBJECT: Data Acquisition, Sept. 17-19 SFP Model Operations

Data recording will commence as soon as possible after instrumentation is hooked up and checked out. There will be a minimum of three runs, each consisting of two hours (6 Dec-tapes) of continuous data recording. During these runs, the model will be tethered to the ELLEN B. SCRIPPS. In addition to computer, analog mag tape and strip chart recording of all data there will be visual and photographic recording of sea and weather conditions, heading and relative angle between model and tether line. A final data run will be attempted with the model in a free drifting mode. Data will be recorded for as long as conditions allow, not exceeding two hours.

Instrumentation will consist of:

10 load cells to measure all loads imposed on the Major Module (MM) by the legs, crosstubes and tether line. (10 channels)

Spiess accelerometer, mounted on the MM to measure accelerations in 3 directions. (3 channels)

Pitch and Roll indicator, mounted on the MM. (2 channels)

Wesmar sensor, mounted on the MM to measure relative motion between MM and sea surface. (1 channel)

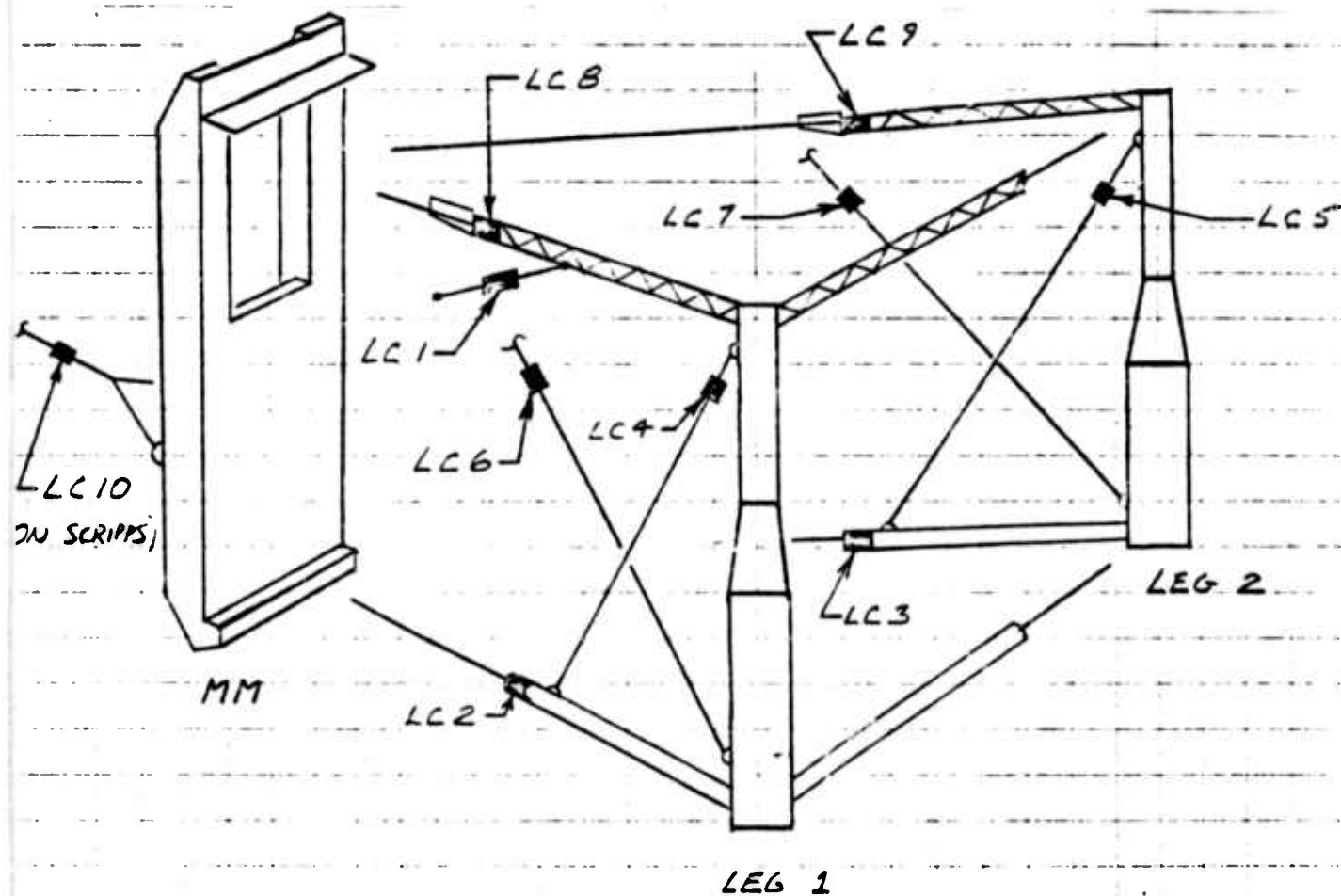
Two vibrotrons, mounted on leg #1, at depths of 10 and 50 feet to record sea state. (2 channels)

OAR wave buoy, tethered close to leg #2, to record sea state. (1 channel)

Two strain gauge accelerometers, one mounted on each leg to measure vertical accelerations. (2 channels)

Of the 21 signals, 20 (excluding the tether line load cell) will be recorded on Dectape by the PDP-8/E computer. All the load cells, the Wesmar, OAR, and the two vibrotrons will be recorded on the 14-channel analog tape recorder. The 8-channel strip-chart recorder will be used primarily to monitor each instrument and check for signal level and quality. The enclosed Figure 1 shows load cell locations.

11<



<u>LOCATION</u>	<u>S/N</u>	<u>AMPLIFIER</u>	<u>DATA LINE</u>
LC1	011	1	1
LC2	005	2	2
LC3	007	3	3
LC4	003	4	4
LC5	008	5	5
LC6	004	6	6
LC7	006	7	7
LC8	012	8	8
LC9	009	9	9
LC10	010	Spare	None

Figure 1. Load Cell Locations

Part II

WAVE BREAKING IN DEEP WATER

Principal Investigator

Dr. W. G. Van Dorn

Phone (714) 453-2000, Extension 1179

Graduate Student

Stephen E. Pazan

Phone (714) 453-2000, Extension 1179

ADVANCED OCEAN ENGINEERING LABORATORY

Sponsored by

ADVANCED RESEARCH PROJECTS AGENCY

STRATEGIC TECHNOLOGY OFFICE

ONR Contract N00014-69-A-0200-6012

Part II
WAVE BREAKING IN DEEP WATER

Table of Contents

	Page
I. Project Summary	1
II. Technical Report	2
III. Future Plans	8
IV. References	8

List of Figures

Figure 1.	Flow direction (arrows) and velocity isolines (cm/sec) for 0.66 Hz wave 2.85 sec (1.9 wavelength) before breaking. Circles indicate surface profile data.	9
Figure 2.	Flow direction (arrows) and velocity isolines (cm/sec) for 0.66 Hz wave at the breaking point. Note that the particle velocities at the crest just exceeds the Stokes limiting phase velocity. Circles and crosses indicate surface profile data.	10
Figure 3.	Flow direction (arrows) and velocity isolines (cm/sec) for 0.66 Hz wave 0.3 sec (0.18 wavelength) after breaking.	11
Figure 4.	Lagrangian streamlines derived from Figs. 1-3.	12
Figure 5.	.66 Hz Stokes wave of limiting form.	13

List of Figures (cont.)

- Figure 6. The (X) marks designate the measured potential energy at a particular station. The solid line indicates the expected growth in energy of the wave due to lateral convergence. 14
- Figure 7. Comparison of dye blob change over a wave period between a low- (a) and near-breaking (b) waves. 15

I. Project Summary

This report summarizes results of the final six months of a two-year laboratory study of the factors controlling breaking of deep water waves, such as occur under storm conditions in the open sea. Although support under this contract terminated December 31, 1973, and because our experiments were not completed until early December, this report includes results from only about one third of all data obtained. Data analysis is continuing under a no-cost contract extension with limited support under separate contract, and the final report of all work will be completed on or before June 30, 1974.

Work during the past six months was divided into two phases. The first phase was a continuation of previous work, examining in greater detail the transformations of internal velocity fields and profiles of periodic waves forcibly "squeezed" to the breaking point within a convergent channel. By comparing consecutive profiles and velocity contour plots, it is apparent that characteristics which distinguish waves approaching the breaking point from symmetric, steady-state, limiting-height waves of the Stokes type are confined to the terminal 80% of wave growth, and to the region beneath the crest above the still water level. Marked asymmetry, leading to a plunging jet, involves very steep velocity gradients within the uppermost 10% of crest height. Crest particle velocities are sometimes accelerated from phase velocity to 60% higher in less than $1/5$ wave period. A brief, but illuminating series of pitchpoling experiments with representative model ship hull forms reveals that pitchpoling can only occur when ship-wave interaction occurs very close to the instant of breaking, and if the wave height exceeds overall hull length. A model discus buoy was successfully prevented from pitchpoling by suspending a weight equal to $1/10$ th its displacement from a central cord five diameters beneath the buoy.

The second phase of our experiments involved interactive breaking of bi-harmonic waves in a non-convergent channel. in which shear flow beneath breaking crests was examined by video-taping shadowgraphs produced by injected dye. It was found that dye blobs in sub-critical, non-breaking waves orbited circularly without much change in shape during a wave period. In steep, near-breaking waves, the dye blob was streaked out along the surface to a length about three times the wave height, and its centroid translated in the wave direction by about half this distance. Despite these intense shearing motions, observations of neutrally buoyant ping-pong balls just beneath the crest revealed little tendency to rotate, although the balls were bodily translated similarly with the dye.

II Technical Report

1. Convergent Breaking

After reviewing the results of experiments conducted during the previous six months, considerable instrument upgrading was indicated to improve repeatability and resolution of measurements. Four additional wave staffs were constructed, permitting three fixed cross-channel staffs and three movable staffs on the instrument cart. To improve phase resolution over that of our earlier experiments, the digital multiplexing rate of data acquisition was increased from 10 Hz to 100 Hz. The labor of data analysis was correspondingly increased. After reinstalling the 80-ft convergent barrier, its terminal section was modified to reduce wave reflections. Modifications were also made to the paddle servo system, and a new fiducial timer was installed.

Having, as expected, detected no uniquely frequency-dependent characteristics among previous data, it was decided to concentrate on examining in better detail the changes in wave profiles and internal velocity fields in uniform trains of heavily breaking 0.66 Hz waves, initially attenuated, as before by a ramp function to procrastinate breaking until the first uniform waves arrived at each measurement station. Triplicate data runs were then conducted at 20 or more velocity probe elevations at each of six stations, four before breaking, one at the break point, and the last slightly beyond. Similar measurements were also made with lightly breaking waves, but only at two stations, because the breaking point was much closer to the wave paddle. Altogether this involved more than 350 reproducible data runs.

Figures 1-3 show representative successive contour plots of the magnitudes and directions of internal fluid velocity vectors within the first uniform wave of a 25-wave sequence. Each plot has superimposed on it the corresponding wave profile from the adjacent digital wave staff. Small phase discrepancies between the staff profiles and the composite velocity data block printed by computer represent arrival time variances of order 0.04 seconds. Although these plots are actually time histories at the indicated times and station distances from the breaking point, the time scales were adjusted according to local phase velocity, so that the profiles are an approximation to wave shape in X-Y space. Each plot comprises about one week of data taking, and includes upwards of 600 data points.

Comparing these plots, it is apparent that wave growth toward (Figs. 1 & 2) and slightly beyond (Fig. 3) the breaking point is characterized by increasing profile asymmetry, tilting of all isolines of constant fluid velocity above the still water level, so as to more nearly parallel the forward wave face, and depression of isolines more deeply beneath the crest. At the breaking point, taken as that instant at which peak crest velocity becomes equal to phase velocity, the isolines just beneath the crest have tilted by almost 45 degrees. From the time scale and isobar spacing, one can approximate the peak normal acceleration of nearly 0.5 g, a value derived theoretically (Ref. 1) for Stokes waves of limiting height. Only 0.3 sec ($1/5$ wave period) later (Fig. 3), the crest isolines have wrapped around to form a horizontal jet, within which the peak particle velocity has increased to 1.6 times phase velocity.

Referring, now, to the small arrows indicating instantaneous fluid direction in these three figures, it can be seen that, except for the small, high-velocity region associated with imminent breaking, the local flow directions are nearly symmetrically disposed about the crest centroids above still water level. By overlaying these distributions it appears that fluid direction suffers much less alteration in steepening waves than does velocity. Such overlays show also that the rearward wave face is remarkably little changed in geometric profile between Figs. 1 and 3, while the forward face everts from convex to concave upward above still water within two wavelengths of breaking.

These changes are more easily apparent in Fig. 4, in which the previous profiles have been reproduced, and "Lagrangian" streamlines were drawn in freehand, with reference to the velocity distributions in Figs. 1-3. At breaking (center), the streamlines appear to wrap around a vortex core, although our data grid is too coarse to resolve more detail. In the post-breaking case (top), the horizontal zone in which the plurality of streamlines become vertical in a reference frame moving at wave speed implies vanishing of relative horizontal particle velocity; decreasing streamline spacing toward the right implies vanishing of fluid pressure at the forward face. Further data analysis should enable us to quantify these characteristics normally hypothesized as conditions for wave breaking.

We can now compare Figure 2 (just breaking) with Fig. 5, which contains a similar set of velocity isolines and directions for a limiting Stokes wave, normalized to the same wave height. The values were computed from equations derived by

Michell (Ref. 2). The Stokes wave, of course, is symmetric about its cusped crest, and the velocity isolines nearly horizontal. Numerical magnitudes and directions coincide fairly closely with those on the rear face of the laboratory wave, and even the profile is roughly the same until fairly close to the crest centroid. However, as can be seen at a glance, the profiles and distribution and magnitudes of internal velocities in the leading (right) sector of the waves are drastically different. An intuitive presumption, now being investigated, is that the limiting Stokes solution would be a reasonable approximation to reality in an ideal experiment, where a wave was converged infinitely slowly toward limiting steady-state equilibrium, but that, where the rate of energy accumulation is significant, any slight perturbation will initiate a positive feedback mechanism that transforms the internal flow field to the observed breaking configuration. Further, the intensity of breaking, as confirmed by comparisons (not shown here) between slightly and heavily breaking waves is probably related to the rate of increase of energy density.

As regards energy and its changes, our velocity measurements were confined to within 30° in phase referenced to the wave crest, so that the average kinetic energies over a wavelength cannot be determined. We have, however, integrated mean-square elevations over a wavelength for the same wave at a plurality of stations between the wave paddle and the breaking point (Fig. 6). Such integrations (dashed line) give the relative potential energy change, which, if conserved and equi-partitioned with kinetic energy, should be proportional to the inverse square of convergence width (solid line). The progressive divergence of these lines suggests that steepening of periodic waves toward the breaking point involves a progressive transformation of potential to kinetic energy. Since the streamlines in Fig. 4 can also be construed as lines of constant kinetic energy, our experiments provide, at least, a qualitative picture of how increasing kinetic energy is redistributed within a steepening wave, and may provide the essential clue to the mechanism of breaking as the transformation from a stable to an unstable flow configuration. At least one possible instability mechanism, resulting from perturbation of corner flow in the immediate vicinity of a cusped crest has been derived theoretically by Price (Ref. 3). but the feedback mechanism leading to flow breakdown remains to be explained deterministically--a principal objective of these experiments.

2. Pitchpoling Experiments

Although not a part of our projected experimental program, advantage was taken of a temporary computer breakdown to employ our facilities for producing convergent deep water breakers to briefly investigate the dynamics of several types of rigid bodies in breaking waves. This subject has considerable application to ship and buoy dynamics, but appears not to have received much scientific attention. In the section on ship dynamics of his forthcoming book (Ref. 4), Dr. Van Dorn reviews historical accounts of pitchpoling, and concludes, from consideration of the maximum probable heights of sea waves and estimates of the statistical incidence of wave breaking as related to sea state, that whole-body rotation should be largely independent of longitudinal stability, and is likely to occur only where the height of a breaking wave exceeds a vessel's overall length.

Accordingly, a series of experiments were conducted, wherein representative wooden ship-shape models in 10-cm length increments were longitudinally exposed to the first of a uniform series of (50 cm, 0.66 Hz) heavily breaking waves, preceded by four or five smaller non-breaking waves. All tests were repeated three times, and were documented by wave staff records and color motion pictures. In brief, these experiments can be summarized as follows:

(a) Because surface particle displacements in waves approaching the breaking point undergo progressively larger net down-wave translations, it was necessary to initially position the models by trial-and-error about two wavelengths from the breaker point towards the paddle in order that their final positions coincided with that of the first breaker at the instant of breaking.

(b) To produce pitchpoling, the initial model positions were critical within about 15 cm, or about .075 wavelengths. Similar translations were observed for a barely-buoyant, waterfilled tennis ball, indicating that they were not solely a function of hull shape.

(c) Pitchpoling invariably occurred for hull lengths shorter than, or equal to, the breaking wave height, and only once for a hull length 10 cm longer.

(d) Pitchpoling is a complicated process, wherein a model first pitched up to an angle of about 45° on an advancing wave front, then slid down-wave in the direction of wave advance until about one third of its length was immersed,

the curling breaker impact then completed the rotation. These effects were substantially independent of whether the models encountered the waves bow- or stern-to the waves.

Similar tests were conducted with a 37-cm dia. x 2 cm thick plywood discus buoy model, with a 20 cm polystyrene mast, with the following results:

- (a) The freely floating buoy, properly positioned, invariably capsized, and sometimes rolled over several times.
- (b) Pitching to 45° without capsize occurred when the buoy was equipped with a weight equal to 5 percent of displacement was hung from a 150-cm string centrally secured to the bottom buoy face.
- (c) When the weight was increased to 10 percent of displacement, the buoy smoothly followed the bulk wave contour, with the heavy breaking jet flowing over its upper surface.

These results are now being further investigated by engineers at Gulf General Dynamics concerned with NOAA buoy survivability in storm seas.

3. Interactive Breaking

As earlier proposed (Ref. 5), our experiments were intended to include profile and velocity field measurements similar to those conducted with convergent breaking, but among waves breaking in the non-convergent 8'x8'x150' wave channel as a result of tape programmed interactions between bi-harmonic and poly-harmonic waves. These experiments were considered essential to bridge the gap between possible anomalous breaking within the convergent zone and the random three-dimension breaking observed in storm seas.

Unfortunately, however, owing to a variety of unanticipated holdups, the convergence experiments were not completed until late November, leaving little time for the latter program. Owing to failure of other contract support to materialize, under which we had hoped to continue our laboratory studies, we instead decided to utilize the remaining month to explore the hypothesis that wave breaking is initiated by the development of a rotational vortex within the strong shear gradient just beneath the crest of a near-breaking wave (Fig. 2).

To this end, a bi-harmonic tape program was written for the wave generator having the form:

$$a = A_1 \cos(\omega_1 t) + A_2 \cos(\omega_2 t),$$

having the constants $A_1 = 2.33A_2$, $\omega_1 = 2\pi/0.66 \text{ sec}^{-1}$ and $\omega_2 = 2\pi/0.8 \text{ sec}^{-1}$. These constants were chosen to produce an anti-node between two plexiglass windows in opposite sides of the wave channel. With the amplitude constants proportionally adjustable, the size of composite waves passing through the anti-node could be varied from arbitrarily small to a plunging breaker 42 cm high. With the far window back-illuminated, sharp shadowgraph images of dye blobs hypodermically injected into the flow field could be videotaped through a translucent screen on the near window, and successive images (identified by a timing light) traced off the videotape on replay.

It was found that, although dye images associated with heavy breaking were quite irregular, there was a systematic change in the character of dye distribution during a wave passage as wave amplitude was increased from small to near-breaking. Figure 7a shows the profile transformations during one wave period of a blob of dye injected just beneath the surface slightly after trough passage in one of a series of 0.66 Hz waves 19 cm high. In small waves the blob undergoes very little distortion or displacement from trough to crest and back again. The same situation is depicted in Fig. 7b for a 26.3 cm near-breaking wave. Here, the blob is translated in the direction of wave motion under the crest, and markedly contracted within the convergence zone on its forward face. A half-period later, the blob has been drawn out into thin sheet about 3 cm thick and 3 wave heights long, and its centroid has been translated about one wave height in the wave direction. These results supplement the above-cited observations of large net, ship model translations during passage of near-breaking waves, and indicate that such waves already contain strong shear gradients under their crests. They also imply a heretofore undescribed near-surface transport mechanism (substantially larger than the theoretical Stokes transport) among steep waves, that may have significance to surficial pollution spreading problems.

The question of rotationality in these experiments was tested--admittedly sketchily--by introducing neutrally buoyant ping-pong balls into similar situations. The balls were painted with equator lines and 90° meridians, so that rotary motions could readily be resolved by eye. None of the balls rotated, although all were translated in a manner similar to

the dye centroids, suggesting that, on a scale of the ball diameter (3 cm), the near-crest motions were irrotational. These observations must be temporized by noting that internal viscous retardation that might inhibit rotation of the fluid-filled balls was not investigated. Further studies are planned.

III. Future Plans

In April 1973 we were advised that support for these investigations would probably be terminated at the end of the year. Accordingly, a supplementary proposal was submitted to the Office of Naval Research in May, providing for continuation of the laboratory studies of interactive breaking, as well as preparation for a field study of storm wave breaking from a drilling tower in the North Sea in Fall 1974. Owing to budget limitations, we were advised in late December that funding would be limited to \$20,000, with the specification that primary emphasis be placed on completion of the Final report of our present study, and that any time remaining be directed toward demonstrating the capability to make accurate and unambiguous flow measurements in very large (circa 80 ft) breaking storm waves, for which our present hot-film techniques are clearly inadequate. We anticipate that the final report will be completed by June 1974, and plan to resubmit the field study proposal for funding in calendar 1975.

IV. References

1. Longuet-Higgins (1963) "The Generation of Capillary Waves by Steep Gravity Waves," JFM, Vol. 16, pp. 138-159.
2. Michell, J. G. (1893) "On the Highest Waves in Water," Philosophical Magazine, Vol. 36, No. 5, pp. 430-435.
3. Price, R. K. (1970) "Detailed Structure of the Breaking Wave," JGR, Vol. 75, pp. 5276-5278.
4. Van Dorn, W. G. (1974) "Oceanography and Seamanship", Dodd, Mead & Co., New York.
5. Van Dorn, W. G. and R. E. Davis (1973) Wave Breaking in Deep Water, AOEL #42, Technical Progress Report, June 30, 1973.

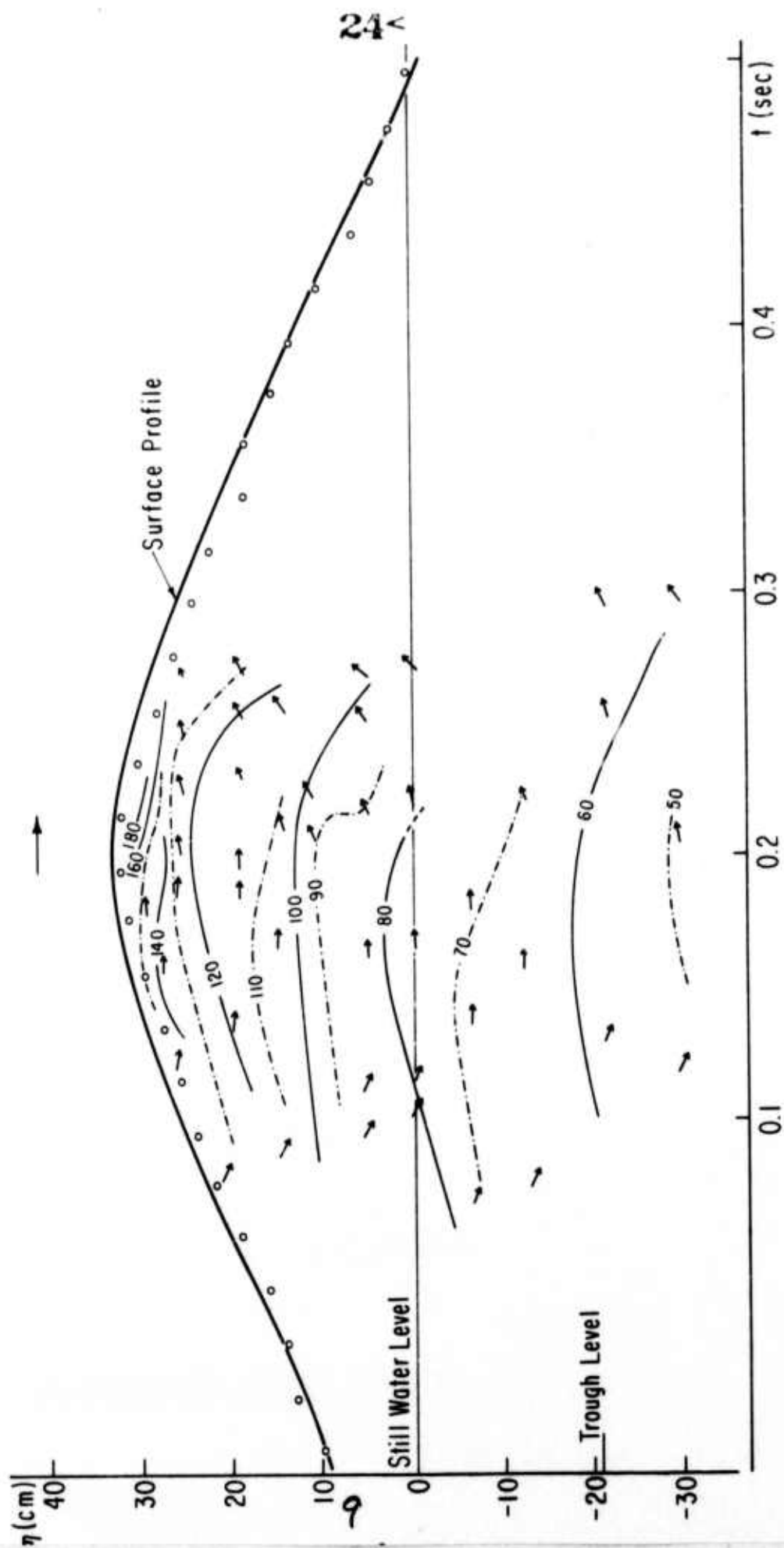


Figure 1. Flow direction (arrows) and velocity isolines (cm/sec) for 0.66 Hz wave 2.85 sec (1.9 wavelength) before breaking. Circles indicate surface profile data.

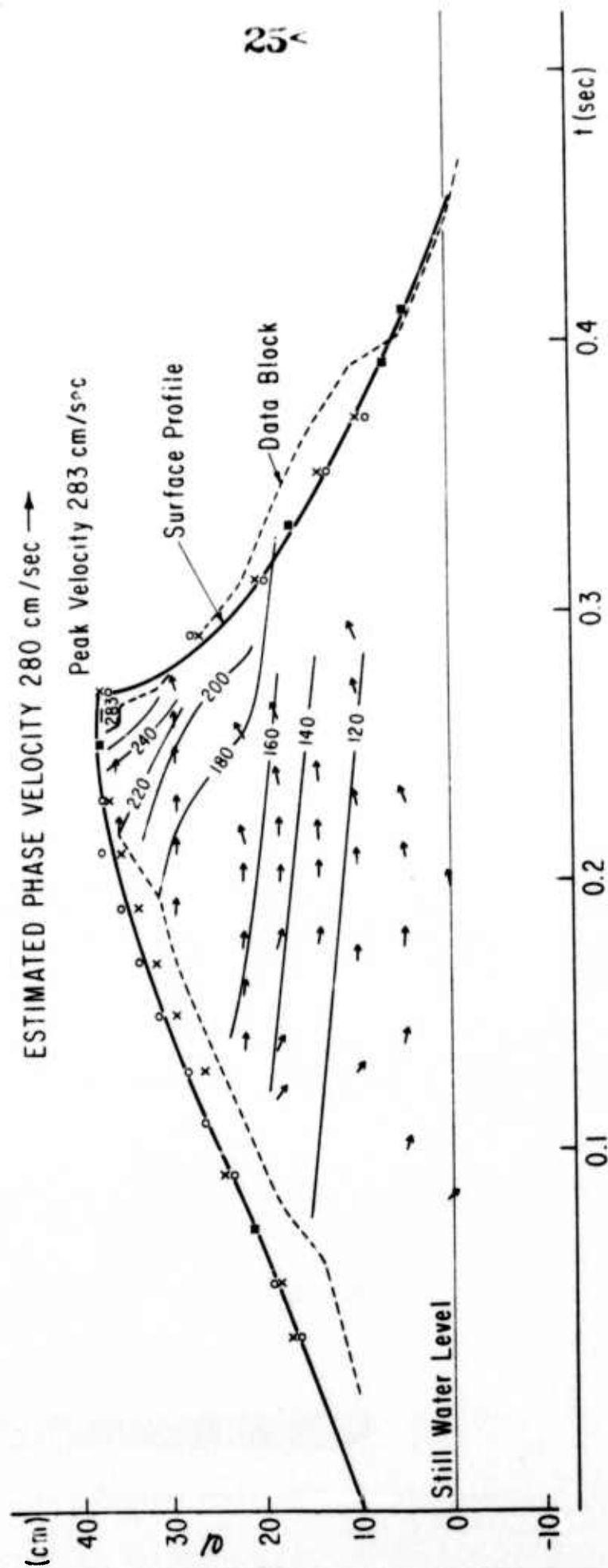


Figure 2. Flow direction (arrows) and velocity isolines (cm/sec) for 0.66 Hz wave at the breaking point. Note that the particle velocities at the crest just exceeds the Stokes limiting phase velocity. Circles and crosses indicate surface profile data.

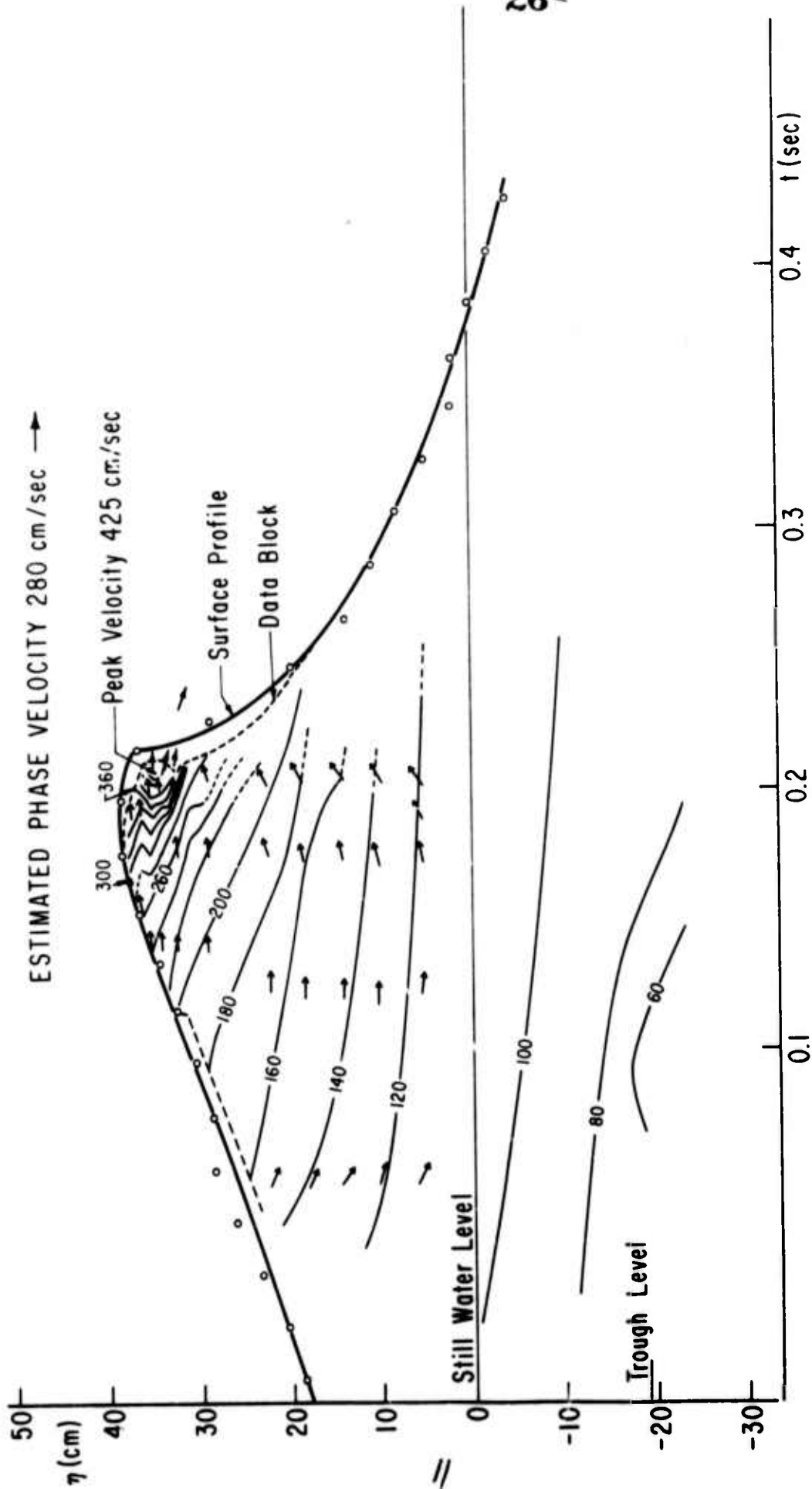
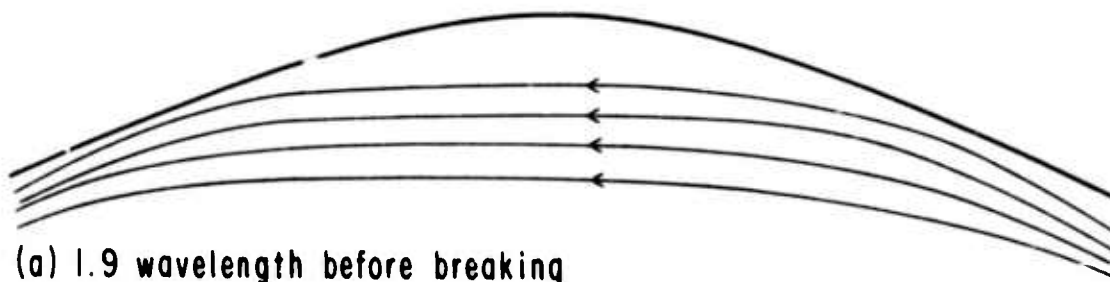
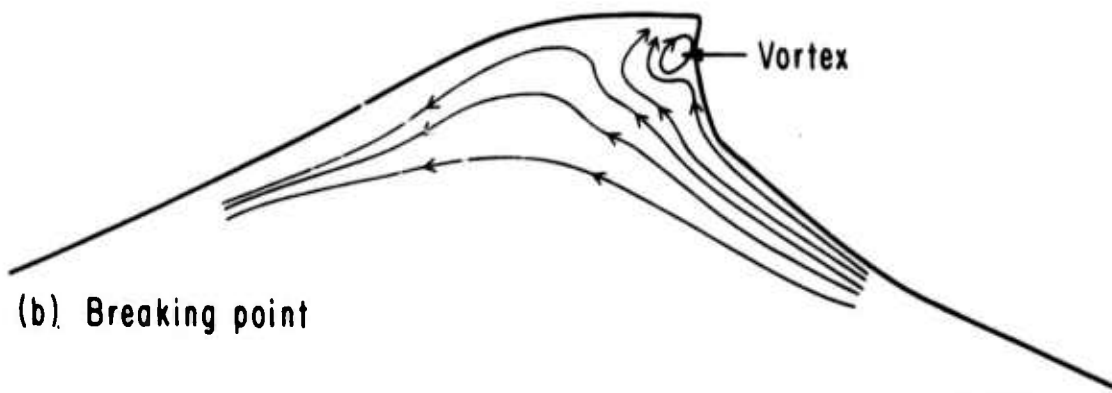


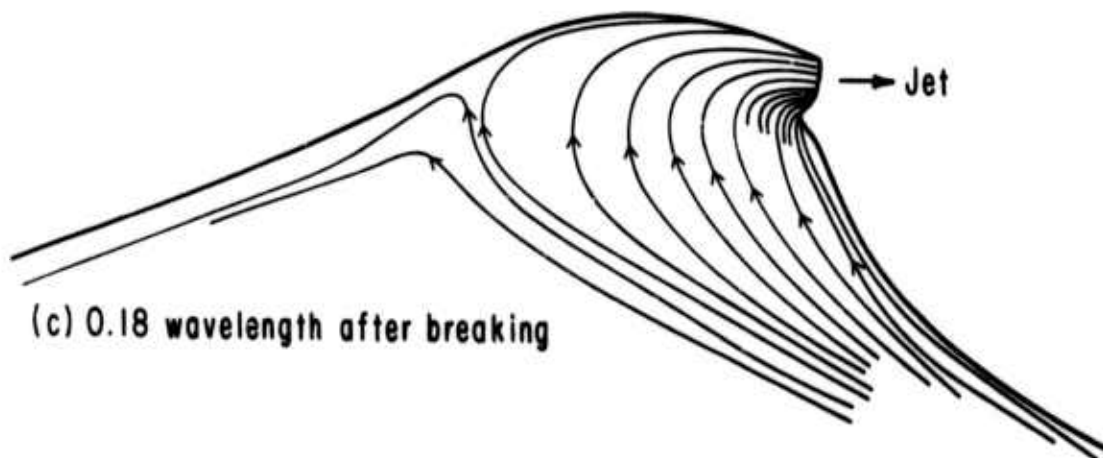
Figure 3. Flow direction (arrows) and velocity isolines (cm/sec) for 0.66 Hz wave 0.3 sec (0.18 wavelength) after breaking.



(a) 1.9 wavelength before breaking



(b) Breaking point



(c) 0.18 wavelength after breaking

Figure 4. Lagrangian streamlines derived from Figs. 1-3.

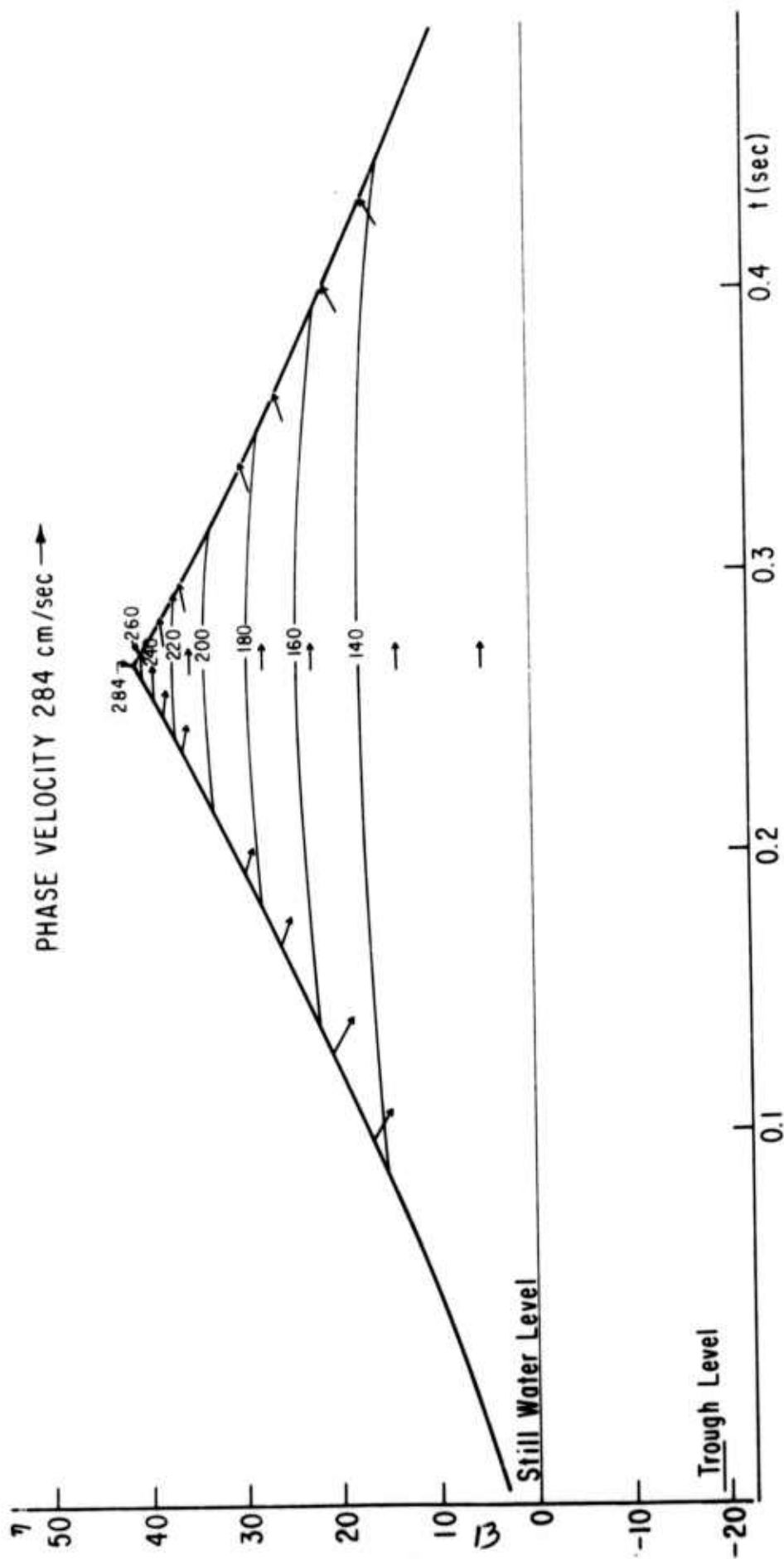


Figure 5. .66 Hz Stokes wave of limiting form.

0.66 Hz HEAVY BREAKING

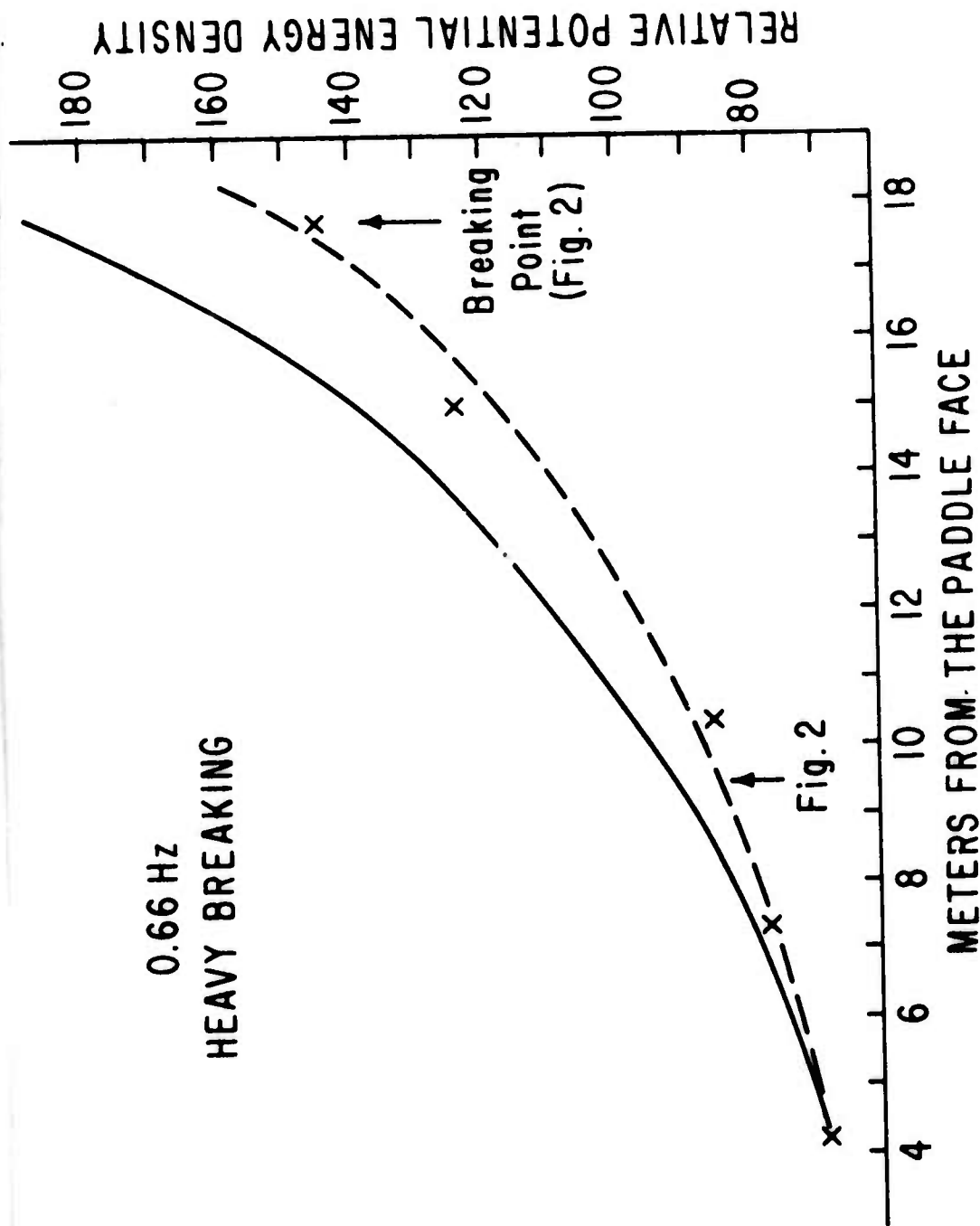


Fig. 6 The (X) marks designate the measured potential energy at a particular station. The solid line indicates the expected growth in energy of the wave due to lateral convergence.

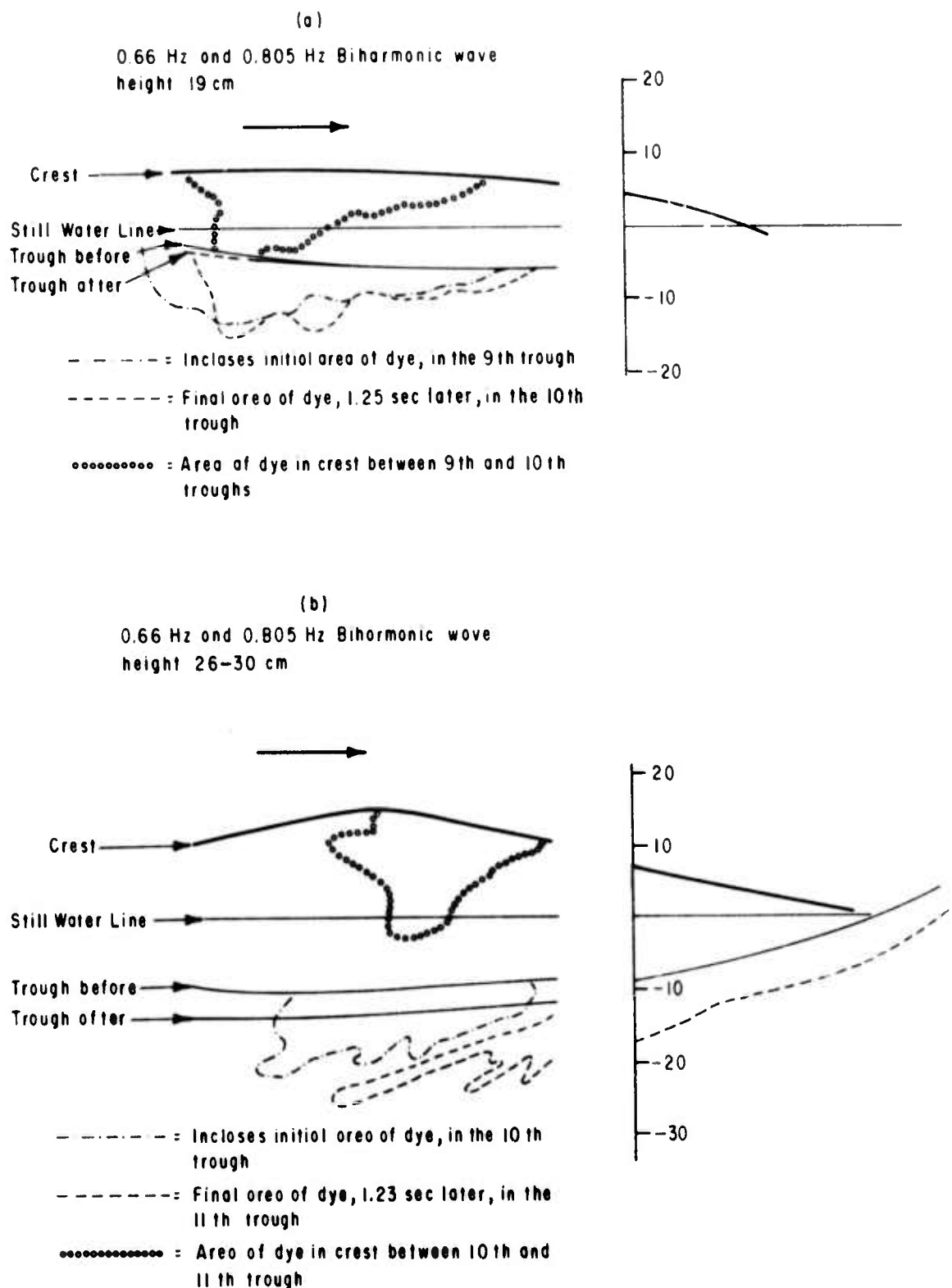


Figure 7. Comparison of dye blob change over a wave period between a low- (a) and near-breaking (b) waves.